This is a preprint of: E. J. Adler and J. R. R. A. Martins, "Aerostructural wing design optimization considering full mission analysis," *2022 AIAA SciTech Forum*, San Diego, CA and online, January 3–7, 2022.
The published article may differ from this preprint and is available at: https://arc.aiaa.org/doi/10.2514/6.2022-0382.

Aerostructural wing design optimization considering full mission analysis

Eytan J. Adler* and Joaquim R. R. A. Martins†
Department of Aerospace Engineering, University of Michigan, Ann Arbor, MI, 48109

In the past, aerostructural optimizations have used a single or small number of analyses in cruise to roughly estimate mission performance. This is accurate enough for long missions where the majority of time is spent near a single flight condition in cruise. But for regional and narrowbody aircraft, the fuel burn in climb is a substantial portion of the block fuel burn—traditional methods do not account for this. This work introduces a new approach: mission-based optimization. This approach gives the optimizer detailed information throughout the mission so the optimizer can optimally trade off performance at different flight conditions. The mission is computed by numerically integrating states such as fuel burn across this mission, satisfying force balance at each integration point, and using a physics-based turbofan model.

I. Nomenclature

L	=	lift
W	=	weight
D	=	drag
T	=	thrust
γ	=	flight path angle (positive for climb)
R	=	mission (or mission segment) range
V	=	flight speed
TSFC	=	thrust-specific fuel consumption
W_i	=	initial weight in a mission (or mission segment)
W_f	=	final weight in a mission (or mission segment)

II. Introduction

Analyzing the interaction between the aerodynamic and structural performance of an aircraft wing is integral to aircraft design. It enables aircraft designers to develop wings that strike the best balance of low weight and high aerodynamic performance—two closely coupled and opposing objectives. Optimization of this aerostructural problem has been thoroughly researched. Haftka [1] was one of the first to investigate the coupled problem, using low-fidelity, physics-based tools. Kennedy et al. [2] accomplish it using Reynolds-averaged Navier–Stokes (RANS) computational fluid dynamics (CFD) and a detailed finite element analysis (FEA) model. The first optimizations used an objective function based on the wing's performance at a single flight condition in cruise. However, this approach often results in poor off-design performance. Multipoint optimization can ameliorate this shortcoming by considering multiple cruise flight conditions when computing the objective [3]. In reality, airlines fly a single aircraft on a wide range of missions. A multi-mission formulation, which uses an objective based on performance on a range of missions, can help optimize an aircraft for off-design missions [4]. Liem et al. [5] apply the multi-mission approach to aerostructural optimization

*Ph.D. Candidate, AIAA Student Member
†Professor, AIAA Fellow

by using a surrogate model to predict performance on a wide range of missions, enabling the use of high-fidelity tools to optimize total cost or fuel burn based on real world usage.

The problem with existing single point, multipoint, and multi-mission aerostructural formulations is that they assume the missions are long enough that the wing's performance in climb and descent is negligible. Since conventional single point and multipoint approaches assume a dominant cruise fuel burn, they are ill-suited to aerostructural optimization with shorter missions where the fuel burn in climb is not negligible. For the design of regional and narrowbody aircraft, including future short-range electric and hydrogen-powered aircraft, a new fuel burn estimation method for aerostructural optimization is necessary to design the best possible wing.

In the case of the single and multipoint optimizations [2, 3], the cruise-dominant fuel burn assumption is necessary because they use the Bréguet range equation to represent the fuel burn of the whole mission. Thus, they use an aerostructural analysis in cruise to compute the lift-to-drag ratio for the equation.

Liem et al.'s [5] multi-mission aerostructural optimization makes the cruise-dominant fuel burn assumption for a different reason. Their approach uses a surrogate model of high-fidelity analyses to numerically integrate a realistic step-climb cruise segment. The surrogate is trained with data only at high Mach numbers. Performing sufficient aerostructural analyses to train the surrogate through all Mach numbers in the mission would be too computationally expensive.

Liem et al. [6] investigate an alternative approach that *could* include climb and descent fuel burn. They numerically integrate the fuel burn across the mission profile, calling a surrogate model to obtain aerodynamic performance at each numerical integration point. The surrogate is trained with 28 aerostructural analyses using a low-cost panel solver for the aerodynamic analysis and a detailed finite element model for the structural analysis. This work does not include thickness-to-chord ratio, sweep, or aspect ratio, which are important design parameters to balance the aerodynamic and structural tradeoff.

Numerical mission analysis has also been coupled with other design optimization problems. Hwang et al. [7] use mission analysis along with the multi-mission approach to maximize an airline's profit by performing coupled aerodynamic shape and mission profile optimization. Jasa et al. [8] study the coupled optimization of mission profile and morphing wing twist during flight by using a numerically-integrated mission in the loop.

This work introduces a new approach for analyzing aerostructural wing designs on missions. It takes advantage of recent developments in fast aerostructural analysis with OpenAeroStruct* [9] and detailed, modular mission analysis with OpenConcept† [10]. This results in a solution that can be easily incorporated into future projects to take advantage of OpenConcept's host of electric aircraft and thermal management modeling capabilities. All codes used in this work are open-source.

This mission-based aerostructural analysis and optimization capability enables comparison against the more traditional single point and multipoint in cruise aerostructural optimization methods. In this paper we show that mission-based aerostructural optimization offers up to 1.3% fuel burn reduction compared to single point and multipoint for missions with short cruise segments. We also propose a modification to the objective function for high-fidelity aerostructural optimization on shorter missions that achieves most of the fuel burn benefit of mission-based optimization but with only one additional function evaluation in climb.

The sections in this paper are the following. Section III discusses the models and methods with subsections describing OpenConcept, OpenAeroStruct, and the coupling of the two. Section IV describes the optimization problems. Section V discusses the results of the optimization, compares them to previous methods, and describes the proposed objective function for high-fidelity aerostructural optimization. Finally, Section VI suggests future work, and Section VII concludes the paper.

III. Models and methods

The aerostructural mission analysis used in this work couples two existing codes: OpenConcept for the mission analysis and OpenAeroStruct for the aerostructural model. Both of these codes are open-source and built on the OpenMDAO framework [11], which enables analysis and optimization of complex systems by harnessing analytic derivatives and the MAUD framework [12]. OpenAeroStruct's aerostructural model is incorporated into OpenConcept with a surrogate model, which offers a speedup compared to OpenConcept calling OpenAeroStruct directly.

*https://github.com/mdolab/openaerostruct

†https://github.com/mdolab/openconcept

A. Mission analysis (OpenConcept)

OpenConcept is a general purpose conceptual aircraft design toolkit. At its core it uses numerical integrators to integrate aircraft states, such as fuel burn, over a customizable mission profile. At each numerical integration point, it selects the correct lift coefficient and engine throttle to balance forces. The model is solved all at once using a Newton solver that takes advantage of the built-in analytic derivatives to converge rapidly. The toolkit can handle complexity ranging from models with a simple parabolic drag polar and propulsion model to models using vortex lattice-based aerodynamics, parallel hybrid engine maps, and unsteady modeling of a battery and electric motor thermal management system.

The OpenConcept model in this work uses a CFM56 engine deck, which is a kriging surrogate of a pyCycle [13] model, and OpenAeroStruct's aerostructural analysis. The aircraft design parameters, such as maximum takeoff weight and wing area, are based on the 737-800's design. Because OpenAeroStruct models only the wing, an estimate for the drag of the rest of the aircraft is required. This is done by matching the fuel burn to an equivalent OpenConcept model with an empirical parabolic drag polar of the 737-800 [14] instead of OpenAeroStruct's. This results in a drag coefficient of 0.0145 that is added to the drag from OpenAeroStruct. The wing weight returned by OpenAeroStruct is added to the OpenConcept model after subtracting the initial wing weight as estimated by Raymer [15].

The mission profile used in all the results discussed this paper is shown in Figure 1. The climb and descent segments have a set profile and the cruise segment is at 35,000 ft and Mach 0.78 for its duration. The climb and descent profiles are roughly based on real-world data from similarly-sized aircraft, though they are still contrived. The cruise segment is unrealistic for the 300 nmi mission since a lower cruise altitude would likely be chosen, and is also unrealistic for longer missions since a step climb would be used as fuel is burned. The idea behind the chosen mission profile is not for it to perfectly represent a real-world mission, but to provide a means for fairly comparing the different optimization methods and in a way that is scalable to an arbitrary distance. Regardless of the mission length, the aircraft takes off at its maximum takeoff weight.

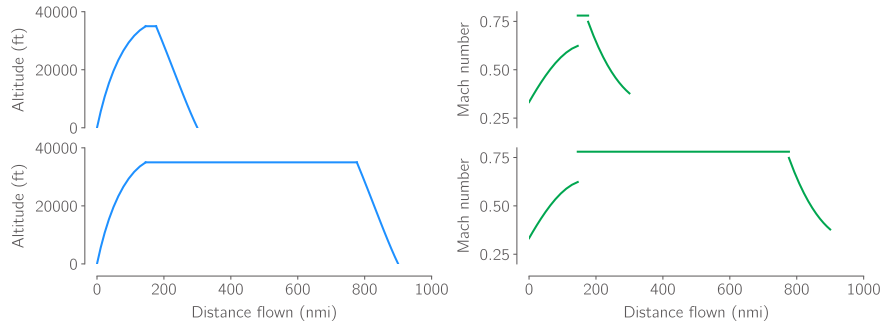

Fig. 1 The mission profile consists of climb, cruise, and descent segments with the cruise at 35,000 ft and at Mach 0.78. The cruise segment is stretched until the mission reaches the desired length. The 300 nmi mission profile is on top, while the 900 nmi mission profile is on the bottom.

B. Aerostructural analysis (OpenAeroStruct)

OpenAeroStruct [9], the aerostructural analysis component, couples a vortex lattice aerodynamic model with a one-dimensional FEA model using six degree-of-freedom elements with axial, bending, and torsional stiffness. In this work we use OpenAeroStruct's wingbox model [16], which computes cross-sectional properties of airfoil-based wingbox cross-sections as opposed to the default tubular cross-section. To account for skin friction and pressure drag, OpenAeroStruct uses a semi-empirical model based on flat-plate estimates and a form factor adjustment. Finally, OpenAeroStruct includes a wave drag estimate based on the Korn equation. While the state-of-the-art in aerostructural optimization uses high-fidelity RANS CFD and a detailed FEA wingbox model, that approach requires thousands of core-hours for a single aerostructural optimization. Despite the lower fidelity, OpenAeroStruct has been shown to match closely with the higher fidelity cases [16]. Since it is capable of aerostructural analysis in seconds, OpenAeroStruct enables rapid mission analysis of the wing and ultimately coupled aerostructural and mission profile optimization on a personal computer.

The wing used in this work, shown in Figure 2, has a simple planform defined by area, aspect ratio, taper, and sweep. The planform area of 124.6 m^2 is the only parameter that is not modified by the optimizer. The wing also has adjustable

twist and thickness-to-chord ratio along the span. The wingbox model's structural sizing consists of skin (same for top and bottom) and spar (same for front and back) thicknesses that are also adjustable along the span. The front of the wingbox is at 10% chord and the rear is at 60% chord. The mesh includes 28 aerodynamic (and structural) panels across the span and 3 aerodynamic panels along the chord. Table 1 lists the parameters used for the wing and wingbox. The weight of the wing structure is added as a distributed load in the finite element model, but no distributed fuel load is included. The model also does not yet include a horizontal stabilizer to trim the aircraft. In the future, these would be useful additions for more accurate results.

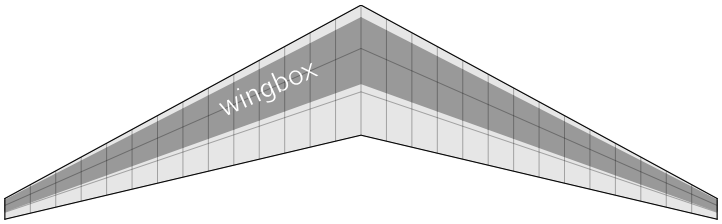

Fig. 2 The baseline wing uses a simple planform with area, aspect ratio, taper, and sweep based on publicly available 737-800 data.

Parameter	Value
Planform area	124.6 m^2
Wingbox shape	10-60% of NACA SC2-0612 airfoil
Young's modulus	73.1 GPa
Shear modulus	27.5 GPa
Yield stress	420 MPa
Safety factor	1.5
Material density	2,780 kg/m^3

Table 1 Structural parameters are based on 7000-series aluminum used in the 737-800 wing.

C. Coupling of mission and aerostructural analyses

While OpenAeroStruct is fast, it is not fast enough to incorporate directly into OpenConcept's mission analysis. An OpenConcept mission uses somewhere on the order of 50 to 100 analysis points throughout the mission for numerical integration. The Newton solver converges this mission in up to 5 iterations. If OpenAeroStruct were included directly, the aerostructural analysis and its derivative computation (a combination of analytic and complex step to compute partial derivatives) would be called hundreds of times. Secondly, if OpenAeroStruct is called directly, the Jacobian in the linear system of OpenMDAO's Newton solver would rapidly become unwieldy. Finally, if this work is to be used in future optimizations, the aerodynamic model may be called tens of thousands of times in a single optimization.

These factors suggest that using a surrogate model would be a good solution. The OpenAeroStruct analyses required to train the surrogate model are easily evaluated in parallel and need only be rerun when the wing design changes. This is also convenient for optimizations without wing design variables since the training data can be generated once at the beginning and then the cheap surrogate can be used throughout.

The surrogate for this model uses SciPy's cubic interpolation [17]. It fits the surrogate quickly and is accurate for this application. If even more accuracy was necessary, particularly at high Mach numbers and angles of attack where there is increased curvature in the drag coefficient, a kriging surrogate model could be considered [5, 6] at the expense of increased surrogate training time. The surrogate model is automatically retrained anytime the wing design changes, but will otherwise use existing data.

The inputs to the surrogate are Mach number, angle of attack, and altitude. Because all possible flight conditions of a mission must be captured, the surrogate is trained with Mach numbers from 0.1 to 0.9, angles of attack from -10 to 15 deg, and altitudes from 0 to 40,000 ft. To better capture the drag rise at high Mach numbers, most of the training points are clustered between Mach 0.7 and 0.9. Overall, the surrogate performs a sweep over nine Mach numbers, six angles of attack, and four altitudes, resulting in 216 aerostructural analyses. These cases run in 40 seconds in parallel on a 16-core

AMD Ryzen 5950X. The surrogate is accurate, estimating fuel burn to within tenths of a percent, so the training grid could be coarsened for further runtime improvements while still closely representing the OpenAeroStruct data.

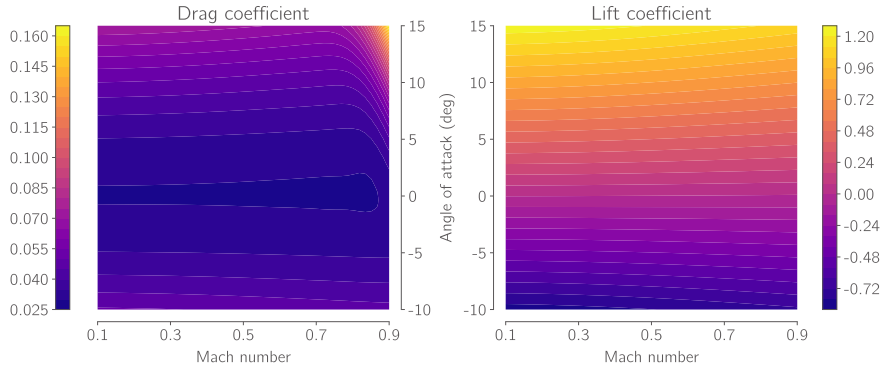

Fig. 3 Drag and lift coefficient surrogate model at 30,000 ft.

D. Surrogate model accuracy

To evaluate the surrogate model's accuracy we compare two separate mission analyses. The first is a mission with the surrogate as the aerodynamic model. The second is a mission with OpenConcept calling OpenAeroStruct directly in the loop. Calling OpenAeroStruct directly comes at the cost of nearly a ten-fold increase in the runtime of a mission analysis, which shows why an accurate surrogate is beneficial for mission analysis and optimization. When trained with 216 aerostructural analyses, the surrogate matches closely to the mission run with OpenAeroStruct directly in the loop. Figure 4 shows the error due to the surrogate model in the 300 nmi mission and Figure 5 shows the same for the 2900 nmi mission. For both cases, the results match the exact values to within a couple tenths of a percent.

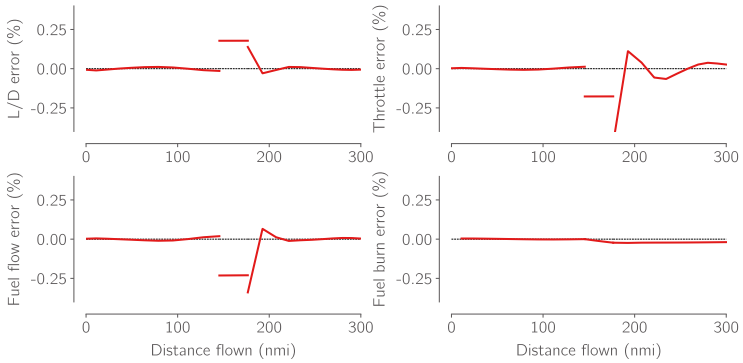

Fig. 4 The surrogate estimates fuel burn to within 0.02% for the 300 nmi mission.

The flight conditions with the greatest error are those at high Mach numbers. This is due to the rapid increase in drag coefficient at high Mach numbers and high angles of attack, which can be seen in Figure 3. Since the 2900 nmi mission spends more time in cruise, which is at Mach 0.78, the error accumulates and results in more error in the fuel burn for the 2900 nmi mission than the 300 nmi mission. The curvature is difficult for the surrogate model to capture, but it still performs well. More advanced surrogate modeling techniques, such as kriging models, could be used to try to better approximate this behavior.

For general purpose use within OpenConcept, estimating fuel burn to within tenths of a percent is more than sufficient. If even more rapid evaluation is necessary or the aircraft being modeled does not fly in the transonic regime, the grid of Mach numbers, angles of attack, and altitudes that is used to train the surrogate can be coarsened.

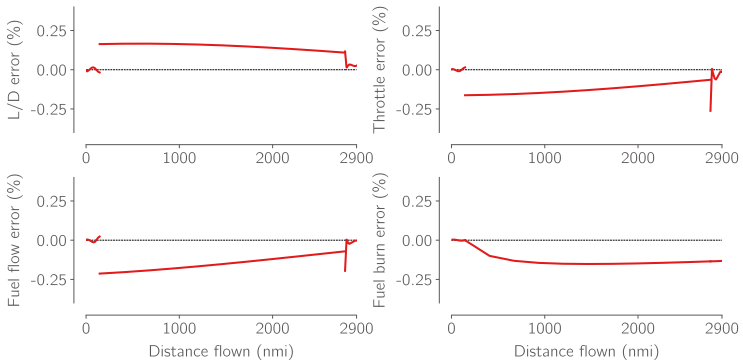

Fig. 5 The 2900 nmi mission has slight more error due to longer durations at high Mach numbers, but still estimates fuel burn to within 0.13%.

IV. Optimization

The mission-based optimization problem, listed in Table 2, is to minimize the fuel burn over the course of the mission by varying the aerostructural wing design. Thanks to the modularity of OpenConcept, this could be easily extended to more complex models or other objective functions, such as direct operating cost. The structure is sized by a 2.5g maneuver condition at 20,000 ft, Mach 0.78, and MTOW to use a similar methodology as Kenway and Martins [3]. The angle of attack to satisfy lift equals weight at the maneuver condition is solved for internally in OpenConcept using the Newton solver. The Kreisselmeier–Steinhauser function is used to aggregate the stress constraints of the wingbox. Aspect ratio is limited to 10.4 to meet the wingspan limit of the Group III gates the 737-800 uses. Thickness-to-chord ratio has a lower bound at 3%, which is only active at the wingtip. Skin and spar thickness are assigned a lower bound of 3 mm, adopted from Chauhan and Martins [16].

	Function/variable	Bound	Note	Quantity
minimize	mission fuel burn		Computed by OpenConcept	
with respect to	aspect ratio	<10.4	Limited for Group III gate wingspan	1
	taper ratio			1
	quarter-chord sweep			1
	wing twist		B-spline interpolated, set to 0 deg at tip	3
	thickness-to-chord ratio	>3%	B-spline interpolated	4
	skin thickness	>3 mm	B-spline interpolated	4
	spar thickness	>3 mm	B-spline interpolated	4
			Total	**18**
subject to	stress at 2.5g < 280 MPa		20,000 ft and Mach 0.78 at MTOW	1
			Total	**1**

Table 2 Mission-based optimization problem

To assess the benefit of mission-based optimization over previous methods, two traditional optimization methods are also included: single point and multipoint in cruise.

Single point optimization, listed in Table 3, estimates fuel burn based on a single aerostructural analysis in cruise. The fuel burn estimate uses the Bréguet range equation at the single point flight condition with a constant thrust-specific fuel consumption value of 17.76 g/(kN-sec). The flight condition of the single point is the cruise flight condition at Mach 0.78 and 35,000 ft with half of the fuel burned. The initial weight is evaluated the same way as mission-based by adding the difference between the new and original wing weights (as estimated by Raymer) to MTOW.

Multipoint optimization, listed in Table 4, is intended to avoid single point's pitfall of improving on-design performance at the cost of worse off-design performance. This multipoint implementation uses the same approach as Kenway and Martins [3], where the design cruise condition is perturbed by Mach 0.01 and 1,000 ft in altitude. This results in five flight conditions, shown in Figure 6. To compute the objective function, fuel burn estimates are computed using the same estimation method as single point for each of the five flight conditions. The average of the five fuel burns becomes the objective.

	Function/variable	Bound	Note	Quantity
minimize	fuel burn		Computed with Bréguet range	
with respect to	aspect ratio	<10.4	Limited for Group III gate wingspan	1
	taper ratio			1
	quarter-chord sweep			1
	wing twist		B-spline interpolated, set to 0 deg at tip	3
	thickness-to-chord ratio	>3%	B-spline interpolated	4
	skin thickness	>3 mm	B-spline interpolated	4
	spar thickness	>3 mm	B-spline interpolated	4
	cruise angle of attack			1
	maneuver angle of attack			1
			Total	**20**
subject to	stress at 2.5g < 280 MPa		20,000 ft and Mach 0.78 at MTOW	1
	cruise L = W		Weight with half of fuel burned	1
	maneuver L = W		Weight at 2.5g	1
			Total	**3**

Table 3 Single point optimization problem

	Function/variable	Bound	Note	Quantity
minimize	fuel burn		Average of five cruise conditions	
with respect to	aspect ratio	<10.4	Limited for Group III gate wingspan	1
	taper ratio			1
	quarter-chord sweep			1
	wing twist		B-spline interpolated, set to 0 deg at tip	3
	thickness-to-chord ratio	>3%	B-spline interpolated	4
	skin thickness	>3 mm	B-spline interpolated	4
	spar thickness	>3 mm	B-spline interpolated	4
	cruise angles of attack			5
	maneuver angle of attack			1
			Total	**24**
subject to	stress at 2.5g < 280 MPa		20,000 ft and Mach 0.78 at MTOW	1
	cruise L = W		Weights with half of fuel burned	5
	maneuver L = W		Weight at 2.5g	1
			Total	**7**

Table 4 Multipoint optimization problem

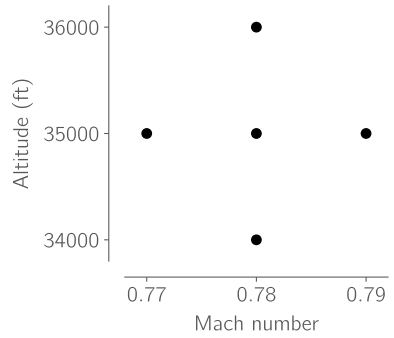

Fig. 6 Multipoint averages fuel burn estimates from five flight conditions for its objective function.

To fairly compare the optimization methods, the resulting wing design from each optimization method is run on the mission profile in OpenConcept calling OpenAeroStruct directly.

V. Discussion

The hypothesized benefit of mission-based optimization is that the less time the aircraft spends in cruise during the mission, the more mission-based optimization will outperform single point and multipoint. To investigate this behavior, we run aerostructural optimizations with the three optimization methods on missions ranging from 300 nmi to 2900 nmi. On the 300 nmi mission the cruise segment is only 31 nmi and a minute fraction of the fuel burn. On the 2900 nmi mission, the cruise segment is over 2600 nmi and dominates the fuel burn.

All optimizations reduced the optimality by at least 3-4 orders of magnitude and achieved a feasibility of 10^{-6}, as defined by SNOPT [18]. The single point cases took roughly 5 min on a single thread. The multipoint optimizations ran for 20-30 min on a single thread. The mission-based optimizations required 90 min to reach the same optimality while running the aerostructural analyses to train the in parallel on all 32 threads of the AMD Ryzen 5950X.

The results from the three optimization methods on the range of mission lengths are shown in Figure 7. Because the mission-based optimization is designing the wing based on the most accurate estimate of mission fuel burn, it always finds a better wing design than both single point and multipoint. This effect is especially noticeable for short missions where the mission-based optimization can properly trade off the wing's low and high speed performance in the different flight segments. Even for missions at the top end of the 737's range, mission-based optimization finds a better design. This is partially because it considers climb and partially because it can account for the variation in angle of attack during cruise. This variation is because the mission profile stays at the same altitude and Mach number for the entire duration of cruise, shown in Figure 8. In reality a stepped climb would be used in cruise to maintain a more constant angle of attack. Nonetheless, the trend shows the benefit of including an accurate mission analysis in the wing design optimization.

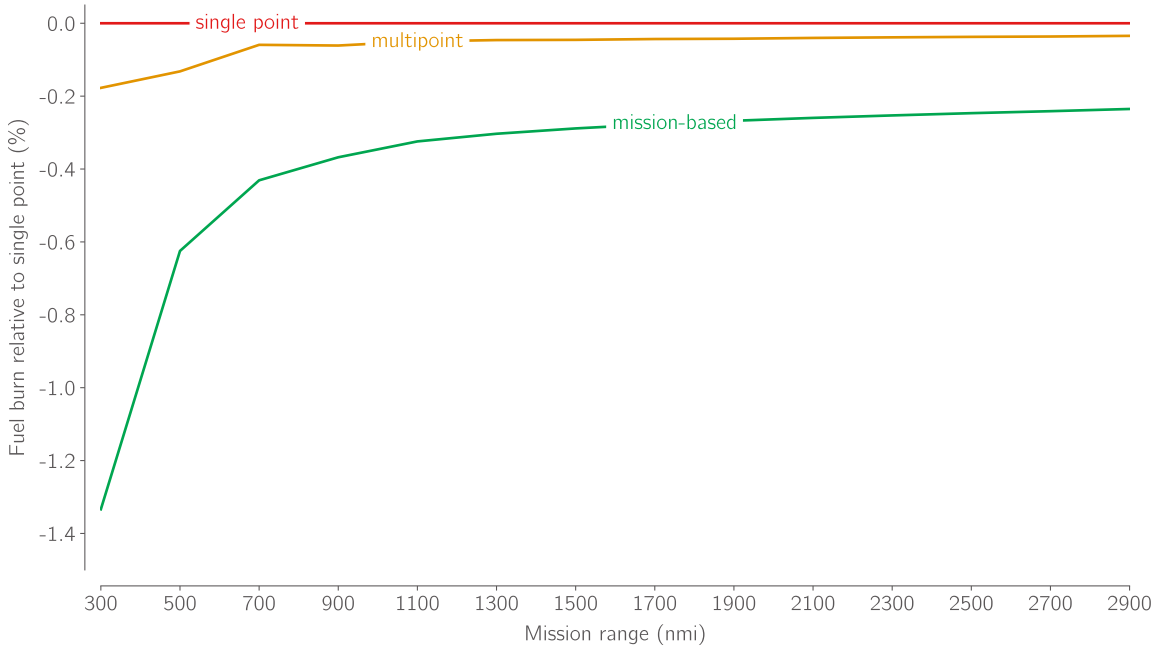

Fig. 7 Mission-based optimization outperforms other conventional methods, particularly for short missions.

By inspecting the relative fuel burn in the mission segments for the mission-based optimized designs, shown in Figure 9, we can understand why mission-based optimization is beneficial. The figure shows that considering performance in climb, and generally in flight segments other than cruise, is critical for these shorter missions. Giving the optimizer a better understanding of how certain decisions affect the performance in every part of the mission enables it to make more informed design choices.

We can see how the mission-based optimization reduces fuel burn relative to the other optimization methods by comparing the wing design. Figure 10 shows the thickness-to-chord ratio and structural thicknesses for wings optimized with the three different methods on the 300 nmi mission. The mission-based optimization identifies that the fuel burn in climb during the 300 nmi mission is much more substantial than fuel burn in cruise. It takes advantage of this knowledge to better optimize the wing for the lower speeds in climb, rather than shaping the wing for the high speed cruise. This manifests as a greater thickness-to-chord ratio than the single point and multipoint cases, allowing it to reduce the

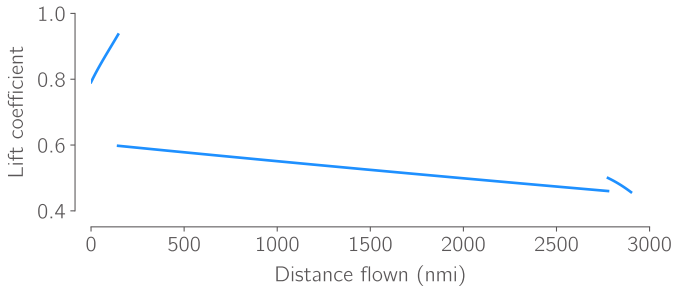

Fig. 8 On long missions, the cruise segment does not stay at the same flight condition because a step climb is not used. This is not a realistic mission profile, but is used because it easily scales to any mission length.

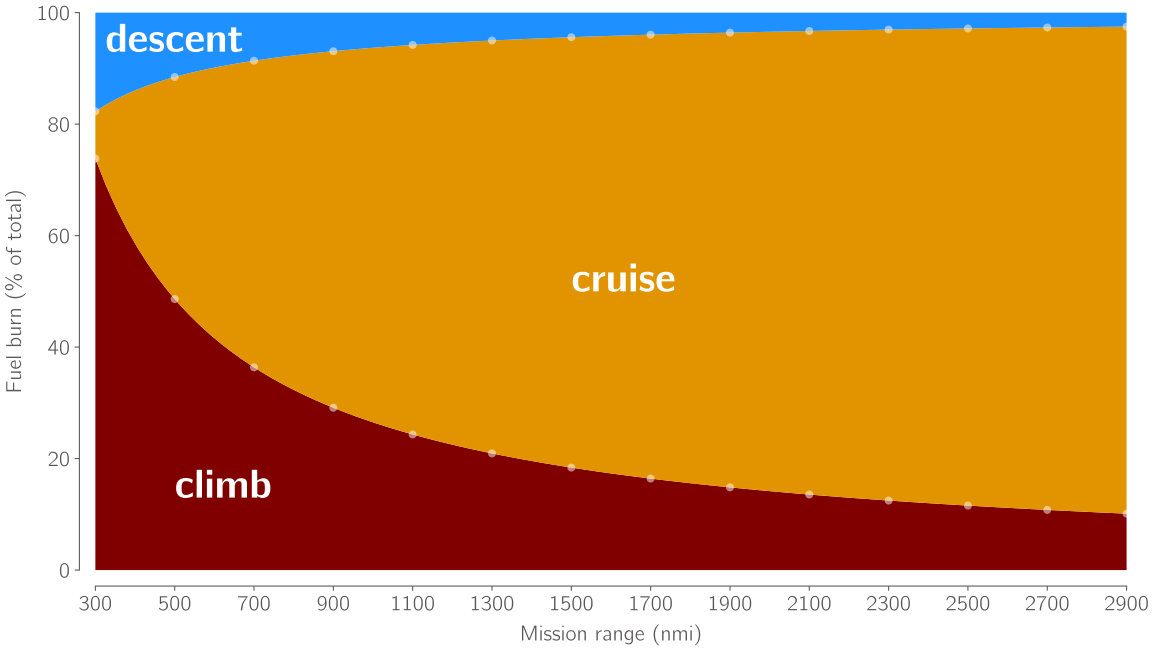

Fig. 9 Fuel burn in climb exceeds cruise fuel burn for shorter missions.

wingbox weight by using thinner spars and skins. Figure 11 shows that mission-based optimization also shifts the lift slightly inboard at the 2.5g structural sizing condition, further enabling a lighter wingbox structure. These results show that thickness-to-chord ratio is an important aerostructural design variable because it is tightly coupled to both aerodynamic (particularly transonic) and structural performance. A smaller thickness-to-chord ratio results in a wing with lower wave drag at the cost of increased weight since it needs a heavier structure to support the bending loads.

Due to the increased thickness-to-chord ratio, the mission-based optimization arrives at a much lighter optimized wing design across all mission ranges. This is a notable result because an aircraft's weight is closely related to its purchase price [19]. Takeoff gross weight has been used as an objective function for aerostructural optimization in the past because of its relationship to both acquisition cost and fuel burn [3, 20].

Figure 12 shows that mission-based optimization returns a wing that is up to 25% lighter than the wing from the other optimization methods. One reason for this is that mission-based optimization can take into account the impact of weight on thrust (and thus fuel burn) when the flight path angle is not zero. The Bréguet range equation assumes that lift equals weight and thrust equals drag. This is not true when the aircraft is climbing or descending since there is a component of weight that acts along the same axis as the thrust. OpenConcept's mission analysis captures this effect. Thus, it is in the interest of mission-based optimization to decrease weight so the climb fuel burn can be reduced.

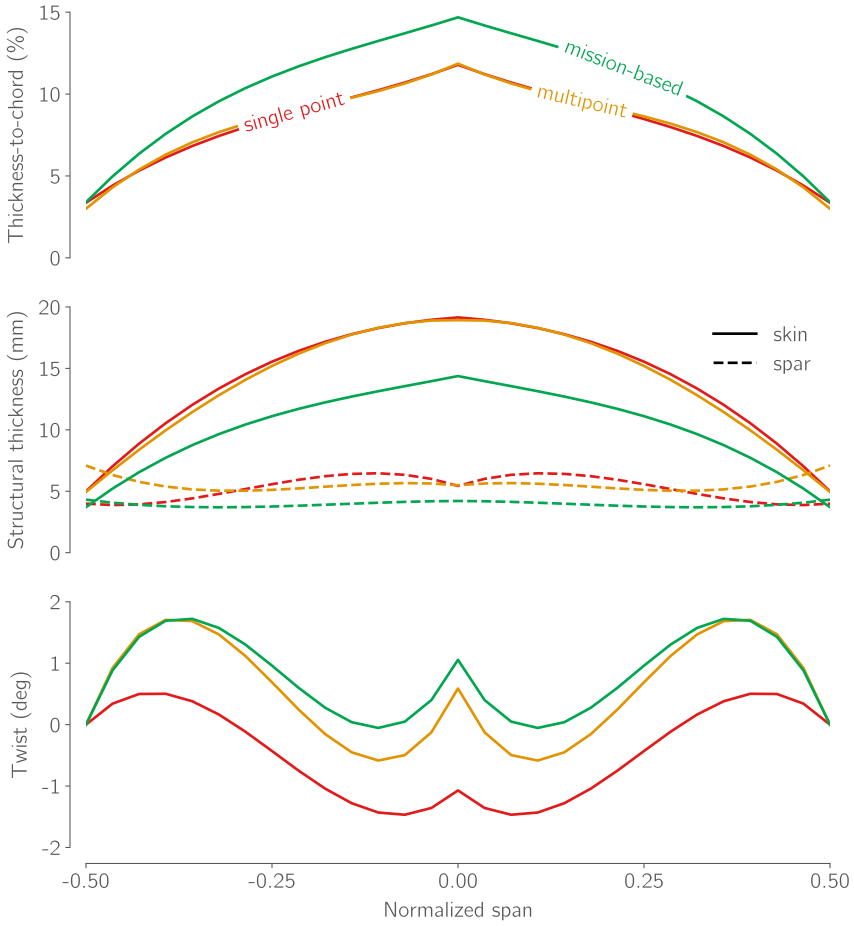

Fig. 10 For the 300 nmi mission, mission-based optimization reduces fuel burn compared to single point and multipoint by increasing the thickness-to-chord ratio, enabling a lighter structure.

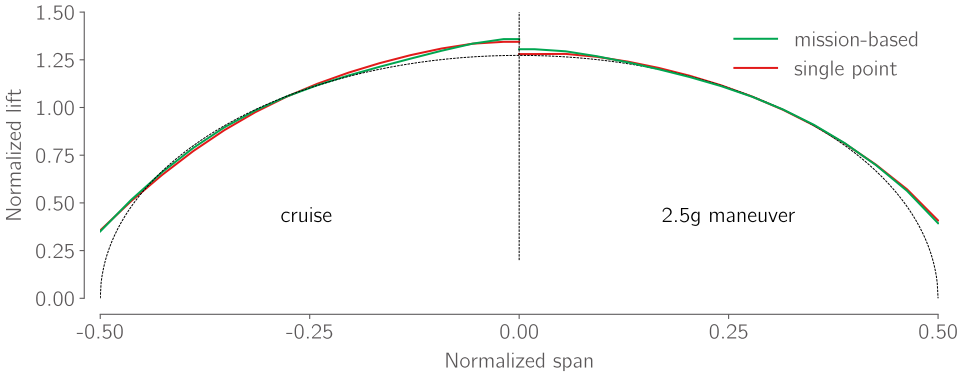

Fig. 11 On the 300 nmi mission, mission-based optimization shifts the lift slightly inboard at the 2.5g sizing condition to decrease the bending moment at the root, further reducing the required structural weight.

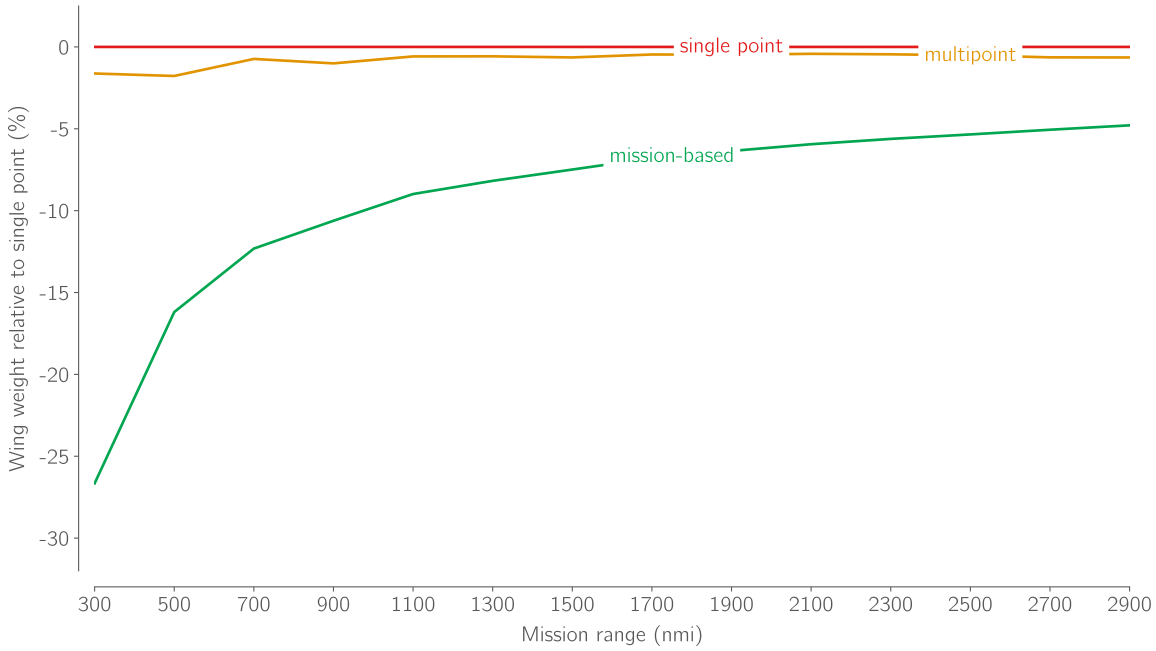

Fig. 12 The wing is much lighter with mission-based optimization than single point or multipoint.

A. Low-cost improvement to single point and multipoint objective function

Motivated by the substantial fuel burn in the climb segment shown in Figure 9 and single point and multipoint's poor modeling of climb, we propose a modification to the traditional fuel burn objective. This approach is an attempt to gain some of the fuel burn improvements of mission-based optimization without the complexity and cost of adding a surrogate and simulating the mission with OpenConcept. Instead of modeling the mission with a single evaluation of the Bréguet range equation, the objective uses two (or more) sequential evaluations of the equation. For this case, we use a single aerostructural analysis in climb and a single one in cruise. Additionally, we modify the Bréguet range equation to satisfy different force balance assumptions that are more accurate for climbing and descending.

The Bréguet range equation assumes lift equals weight and thrust equals drag. In climb and descent weight is decomposed into components that affect both equations as

$$L = W\cos\gamma$$
$$T = D + W\sin\gamma$$

where γ is the flight path angle (positive is climb). By incorporating these assumptions into the range equation derivation, we find the climb and descent range equation:

$$R = \frac{1}{\frac{\cos\gamma}{\frac{L}{D}} + \sin\gamma}\frac{V}{\text{TSFC}}\ln\frac{W_i}{W_f} \tag{1}$$

When the flight path angle is zero, this reduces to the Bréguet range equation. The assumptions of constant lift-to-drag ratio and thrust-specific fuel consumption are less reasonable for climb and descent where the flight conditions vary, but the equation still provides a substantial improvement over the original equation. Since commercial aircraft climb angles are on the order of 2-4 degrees, the small angle approximation can be used here. Fuel burn is computed by manipulating Equation 2 to solve for $W_i - W_f$. The result is

$$\text{fuel burn} = W_i - W_f = W_f\left\{\exp\left[\left(\frac{1}{\frac{L}{D}} + \gamma\right)\text{TSFC}\frac{R}{V}\right] - 1\right\} \tag{2}$$

Though it could be included, we ignore fuel burn in descent since it is small compared to climb and cruise fuel burn (as seen in Figure 9) and would require an additional aerostructural analysis. The procedure used to compute the fuel burn at the end of the cruise segment is the following:

1) Perform an aerostructural analysis at the flight condition halfway through climb.
2) Use Equation 2 to compute the fuel burn in climb.
3) Perform an aerostructural analysis halfway through the cruise segment.
4) Use Equation 2 (in this case with $\gamma = 0$, which simplifies to Bréguet range) to compute fuel burn in cruise. The initial weight, W_i, for this cruise segment calculation is the final weight, W_f, from the climb fuel burn calculation.
5) Compute the objective function as the sum of the fuel burns from the climb and cruise segments (or the initial climb weight minus the final cruise weight).

The optimizer is used to find the angles of attack to satisfy lift equals weight for the two aerostructural analyses. The climb analysis assumes half of fuel weight computed in step 2 has been burned. The cruise analysis uses a fuel weight with the climb fuel and half of the cruise fuel burned. Note that since the cruise aerostructural analysis does not use information from the climb analysis directly, steps 1 and 3 can be done in parallel. Other than the new fuel burn objective and lift equals weight constraint, the optimization problem is the same as the single point optimization problem described in Table 3.

This approach is flexible, so it could be incorporated with a multipoint cruise segment or a mission profile with more segments. For example, a multipoint cruise could be included by using the same calculation for climb fuel burn, but then average the cruise fuel burn (steps 3 and 4) from a handful of different cruise flight conditions.

These optimizations achieved the same optimality and feasibility tolerances as the previous optimizations. They achieved these tolerances after running for 10-15 min on a single thread.

To assess the benefit of using this approach we revisit the same plots as before, but now including optimizations with the new objective. Figure 13 shows the fuel burn of the four objective functions relative to the single point optimization. The new objective function that includes an analysis in climb performs better than both single point and multipoint. Most notably it finds a much better design for the shorter missions than single point and multipoint, which are oblivious to the different flight conditions in climb. The new objective still does not perform as well as mission-based optimization. This should not be surprising because OpenConcept provides a more accurate mission analysis model.

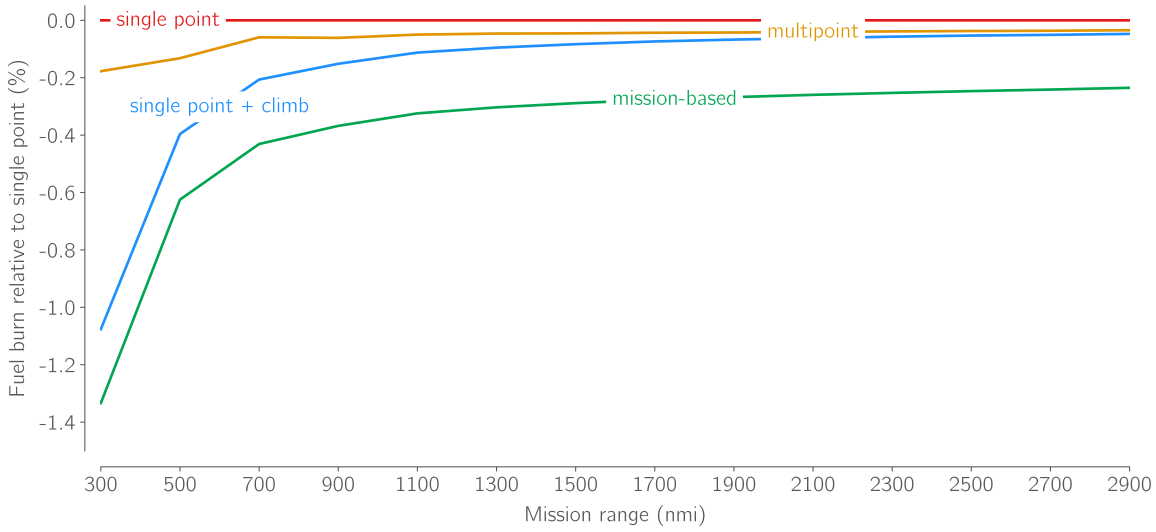

Fig. 13 Including the climb point provides significant improvements over single point and multipoint especially for short missions, but it still does not outperform mission-based.

The proposed objective function achieves similar wing weight reduction to mission-based optimization. Figure 14 shows that for the shorter missions, the new objective (single point + climb) actually returns a lighter wing than mission-based optimization. These weight savings are because the climb fuel burn calculation (Equation 2) includes a component of weight that opposes thrust in its assumptions, making it more sensitive to weight than the traditional Bréguet equation.

To see where these benefits from the new objective function are coming from, we can look at how closely the fuel burn approximations from the four optimization methods match the exact fuel burn computed with OpenConcept calling OpenAeroStruct directly. Figure 15 demonstrates the improvement from adding a climb fuel burn analysis. For short missions the error in the new fuel burn estimate is less than 15% lower than the true mission fuel burn, whereas the single point estimate is over 35% lower. The constant error across all mission ranges is due to the error in Bréguet range's estimate of the cruise fuel burn. This could be due to the variation in the cruise flight condition for longer missions, shown in Figure 8, since a step climb is not used.

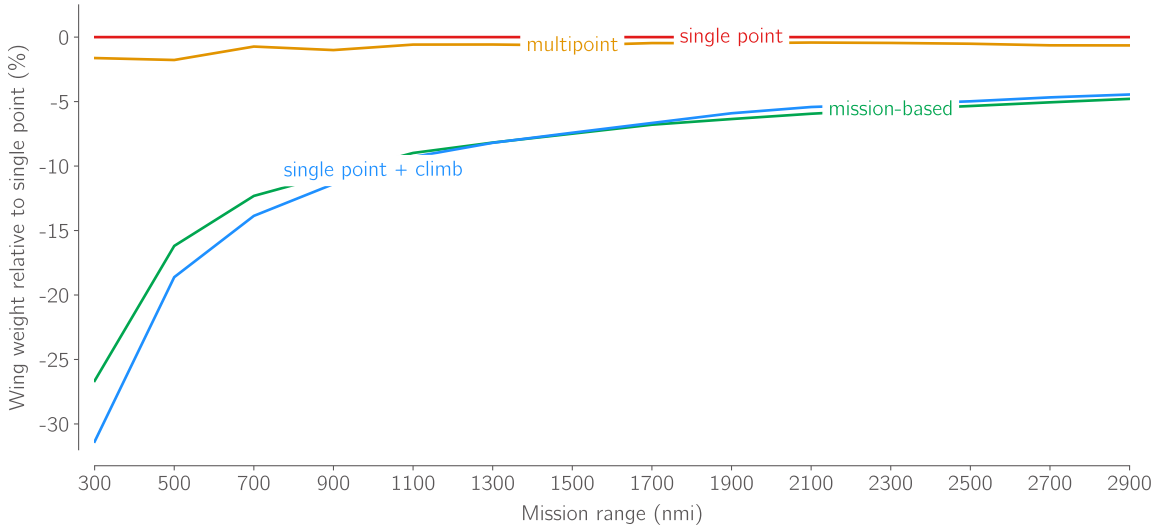

Fig. 14 The proposed objective function achieves similar wing weight benefits to mission-based optimization.

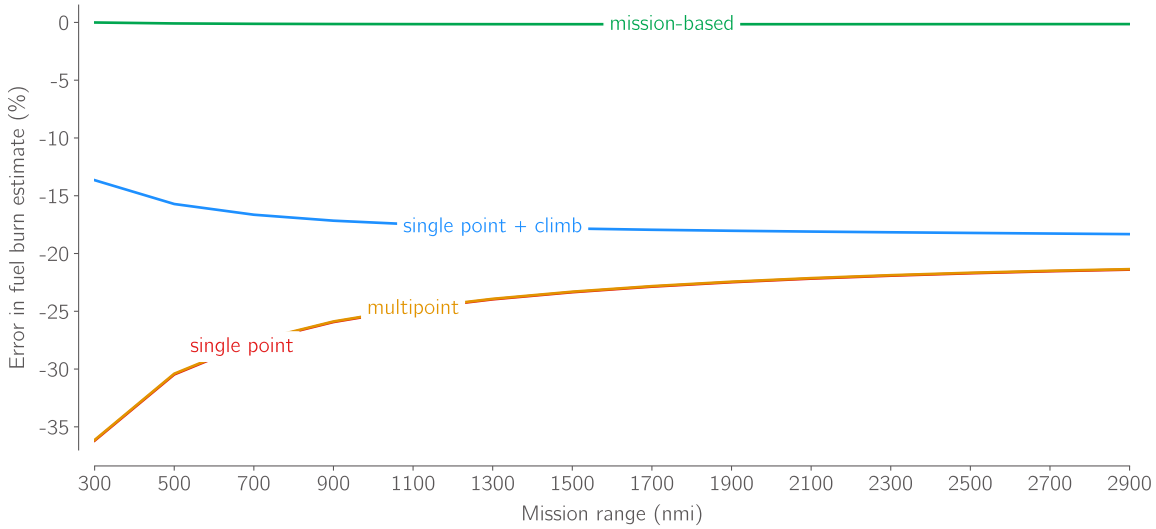

Fig. 15 The new method better approximates the true fuel burn compared to single point. For this figure, a fuel burn estimation in descent for single point + climb is included for a fair comparison between the methods.

VI. Future work

This work does not include the drag from a horizontal stabilizer required to trim the aircraft and to provide longitudinal stability. It also neglects the load alleviation from fuel stored in the wings. Both of these may affect the final wing design and it would be interesting to determine their impact. Another area for work is investigating a more careful selection of training points and a surrogate modeling approach to better predict performance at high Mach numbers.

VII. Conclusions

This work demonstrates the benefits of accurately modeling the mission and its fuel burn in an aerostructural optimization. Giving the optimizer this detailed mission performance model enables it to make more informed decisions that optimally trade off between performance at different flight conditions for a given mission profile.

This mission-based optimization approach is applied to a Boeing 737-sized airplane for mission ranges from 300 nmi to 2900 nmi. For shorter missions with substantial fuel burn in climb, mission-based optimization returns a wing with 1.3% less fuel burn than the wings returned by single point and multipoint optimization. It identifies the benefit of a thicker wing with a lighter structure despite the additional wave drag. The wing designed by the mission-based optimization is up to 25% lighter than the single point and multipoint wings, reducing the aircraft purchase price.

Finally, we propose a new objective function that accounts for the fuel burn in climb with only one more aerostructural analysis than the single point case. Its optimized design burns less fuel and weighs less than both single point and multipoint optimizations for all mission distances. Mission-based optimization still outperforms this new objective because it gives the optimizer the most accurate model of the objective function.

This implementation of mission-based optimization in OpenConcept and OpenAeroStruct is open-source and extensible. OpenConcept's analysis tools introduce the possibility of using mission-based aerostructural optimization coupled with electric and hybrid propulsion, mission profile optimization, a wide range of aircraft, and more.

Appendix

Tables 5, 6, and 7 optimization result data for the 300, 1500, and 2900 nmi missions. The spline control points for the twist, thickness-to-chord, spar thickness, and skin thickness design variables are ordered from values at the tip of the wing to the root. The twist control point at the tip is locked at 0 deg to prevent rigid body motion. The arrays in the multipoint cruise angle of attack and cruise L = W rows are ordered as follows:

1) Mach 0.78, 35,000 ft
2) Mach 0.79, 35,000 ft
3) Mach 0.77, 35,000 ft
4) Mach 0.78, 34,000 ft
5) Mach 0.78, 36,000 ft

		Unit	Lower	Upper	Single point	Multipoint	Mission-based	Single point + climb
minimize	mission fuel burn	kg			2770.44	2765.53	2733.49	2740.63
w.r.t.	aspect ratio			10.401	**10.401**	**10.401**	**10.401**	**10.401**
	taper ratio				0.168	0.174	0.180	0.180
	quarter-chord sweep	deg			23.046	23.524	21.577	21.754
	twist	deg			[0.000, 2.072, -2.862, -1.072]	[0.000, 5.274, -3.630, 0.588]	[0.000, 4.997, -2.787, 1.055]	[0.000, 4.084, -1.460, 1.206]
	thickness-to-chord ratio		0.030		[0.034, 0.086, 0.090, 0.118]	[**0.030**, 0.096, 0.085, 0.119]	[0.034, 0.112, 0.123, 0.147]	[0.038, 0.117, 0.136, 0.157]
	spar thickness	mm	3.000		[3.990, **3.000**, 8.722, 5.434]	[7.088, **3.000**, 6.438, 5.490]	[4.313, **3.000**, 4.177, 4.206]	[3.431, **3.000**, 3.788, 4.058]
	skin thickness	mm	3.000		[4.997, 14.940, 18.469, 19.150]	[4.943, 13.349, 19.230, 18.926]	[3.701, 11.204, 12.398, 14.375]	[**3.000**, 10.435, 11.306, 13.701]
	maneuver angle of attack	deg			11.915	10.445	—	8.866
	cruise angle of attack	deg			8.76	[7.72, 7.54, 7.91, 7.38, 8.07]	—	6.44
	climb angle of attack	deg			—	—	—	9.493
subject to	2.5g failure			0.000	**2.8e-06**	**1.3e-07**	**9.1e-08**	**6.2e-08**
	maneuver L = W		0.000	0.000	**1.8e-08**	**-4.4e-09**	—	**-4.4e-10**
	cruise L = W		0.000	0.000	**1.6e-08**	[**-4.7e-09**, **-4.8e-09**, **-4.7e-09**, **-4.8e-09**, **-4.7e-09**]	—	**-1.4e-10**
	climb L = W		0.000	0.000	—	—	—	**-8.3e-11**

Table 5 Optimization results for the 300 nmi mission

		Unit	Lower	Upper	Single point	Multipoint	Mission-based	Single point + climb
minimize	mission fuel burn	kg			11173.83	11168.74	11141.58	11164.54
w.r.t.	aspect ratio			10.401	**10.401**	**10.401**	**10.401**	**10.401**
	taper ratio				0.155	0.162	0.158	0.161
	quarter-chord sweep	deg			22.447	22.747	22.674	23.070
	twist	deg			[0.000, 5.138, -3.695, 0.393]	[0.000, 5.130, -3.615, 0.490]	[0.000, 4.616, -3.828, 0.185]	[0.000, 5.078, -3.327, 0.678]
	thickness-to-chord ratio		0.030		[**0.030**, 0.096, 0.088, 0.114]	[**0.030**, 0.094, 0.088, 0.115]	[**0.030**, 0.093, 0.093, 0.119]	[0.030, 0.100, 0.093, 0.123]
	spar thickness	mm	3.000		[7.594, **3.000**, 6.046, 5.668]	[5.704, 3.734, 6.020, 5.612]	[7.509, **3.000**, 5.594, 5.102]	[6.219, **3.000**, 5.679, 5.215]
	skin thickness	mm	3.000		[6.298, 13.047, 18.391, 18.897]	[5.727, 13.382, 18.183, 18.891]	[6.081, 12.778, 16.670, 17.185]	[5.248, 12.492, 16.812, 17.560]
	maneuver angle of attack	deg			10.848	10.382	—	10.132
	cruise angle of attack	deg			7.40	[7.37, 7.19, 7.55, 7.04, 7.71]	—	7.04
	climb angle of attack	deg			—	—	—	10.514
subject to	2.5g failure			0.000	**1.4e-06**	**2.1e-08**	**4.6e-08**	**1.4e-07**
	maneuver L = W		0.000	0.000	**-1.2e-09**	**-3.1e-10**	—	**6.9e-09**
	cruise L = W		0.000	0.000	**1.8e-08**	[**1.5e-10**, **1.3e-10**, **1.6e-10**, **1.2e-10**, **1.7e-10**]	—	**6.7e-09**
	climb L = W		0.000	0.000	—	—	—	**6.2e-09**

Table 6 Optimization results for the 1500 nmi mission

		Unit	Lower	Upper	Single point	Multipoint	Mission-based	Single point + climb
minimize	mission fuel burn	kg			20345.36	20338.33	20297.51	20335.74
w.r.t.	aspect ratio			10.401	**10.401**	**10.401**	**10.401**	**10.401**
	taper ratio				0.140	0.146	0.137	0.145
	quarter-chord sweep	deg			21.496	21.853	21.271	21.785
	twist	deg			[0.000, 4.786, -3.656, 0.172]	[0.000, 4.797, -3.647, 0.262]	[0.000, 4.033, -3.943, -0.257]	[0.000, 4.821, -3.388, 0.391]
	thickness-to-chord ratio		0.030		[0.031, 0.096, 0.086, 0.112]	[0.032, 0.092, 0.089, 0.112]	[**0.030**, 0.092, 0.088, 0.113]	[0.031, 0.099, 0.088, 0.117]
	spar thickness	mm	3.000		[6.391, 3.306, 6.034, 5.696]	[6.394, **3.000**, 6.172, 5.660]	[8.009, **3.000**, 5.828, 5.278]	[6.057, **3.000**, 5.989, 5.415]
	skin thickness	mm	3.000		[7.025, 12.508, 18.246, 18.500]	[6.311, 13.303, 17.558, 18.604]	[7.742, 12.004, 17.329, 17.144]	[6.277, 12.110, 17.510, 17.664]
	maneuver angle of attack	deg			10.851	10.410	—	10.193
	cruise angle of attack	deg			7.10	[7.09, 6.92, 7.26, 6.78, 7.42]	—	6.78
	climb angle of attack	deg			—	—	—	10.614
subject to	2.5g failure			0.000	**3.3e-07**	**1.3e-08**	**2.0e-06**	**8.1e-09**
	maneuver L = W		0.000	0.000	**1.0e-09**	**-5.6e-10**	—	**-2.3e-10**
	cruise L = W		0.000	0.000	**-5.3e-09**	[**-3.0e-10**, **-3.2e-10**, **-2.9e-10**, **-3.2e-10**, **-2.8e-10**]	—	**-1.8e-10**
	climb L = W		0.000	0.000	—	—	—	**-1.4e-10**

Table 7 Optimization results for the 2900 nmi mission

Acknowledgments

The first author is supported by the Department of Defense (DoD) through the National Defense Science and Engineering Graduate (NDSEG) Fellowship Program. The first author would like to thank Alasdair Gray for his insightful comments and suggestions.

References

[1] Haftka, R. T., "Optimization of flexible wing structures subject to strength and induced drag constraints," *AIAA Journal*, Vol. 15, No. 8, 1977, pp. 1101–1106.

[2] Kennedy, G. J., Kenway, G. K. W., and Martins, J. R. R. A., "High Aspect Ratio Wing Design: Optimal Aerostructural Tradeoffs for the Next Generation of Materials," *Proceedings of the AIAA Science and Technology Forum and Exposition (SciTech)*, National Harbor, MD, 2014. https://doi.org/10.2514/6.2014-0596.

[3] Kenway, G. K. W., and Martins, J. R. R. A., "Multipoint High-Fidelity Aerostructural Optimization of a Transport Aircraft Configuration," *Journal of Aircraft*, Vol. 51, 2014, pp. 144–160. https://doi.org/10.2514/1.C032150.

[4] Cai, Y., Rajaram, D., and Mavris, D. N., "Multi-mission multi-objective optimization in commercial aircraft conceptual design," *AIAA Aviation 2019 Forum*, 2019, p. 3577.

[5] Liem, R. P., Kenway, G. K., and Martins, J. R., "Multimission aircraft fuel-burn minimization via multipoint aerostructural optimization," *AIAA Journal*, Vol. 53, No. 1, 2015, pp. 104–122.

[6] Liem, R. P., Mader, C. A., Lee, E., and Martins, J. R. R. A., "Aerostructural design optimization of a 100-passenger regional jet with surrogate-based mission analysis," *2013 Aviation Technology, Integration, and Operations Conference*, 2013. https://doi.org/10.2514/6.2013-4372.

[7] Hwang, J. T., Jasa, J. P., and Martins, J. R., "High-fidelity design-allocation optimization of a commercial aircraft maximizing airline profit," *Journal of Aircraft*, Vol. 56, No. 3, 2019, pp. 1164–1178.

[8] Jasa, J. P., Hwang, J. T., and Martins, J. R., "Design and trajectory optimization of a morphing wing aircraft," *2018 AIAA/ASCE/AHS/ASC Structures, Structural Dynamics, and Materials Conference*, 2018, p. 1382.

[9] Jasa, J. P., Hwang, J. T., and Martins, J. R. R. A., "Open-source coupled aerostructural optimization using Python," *Structural and Multidisciplinary Optimization*, Vol. 57, No. 4, 2018, pp. 1815–1827. https://doi.org/10.1007/s00158-018-1912-8.

[10] Brelje, B. J., and Martins, J. R. R. A., "Development of a Conceptual Design Model for Aircraft Electric Propulsion with Efficient Gradients," *2018 AIAA/IEEE Electric Aircraft Technologies Symposium*, Cincinnati, OH, 2018.

[11] Gray, J. S., Hwang, J. T., Martins, J. R. R. A., Moore, K. T., and Naylor, B. A., "OpenMDAO: An Open-Source Framework for Multidisciplinary Design, Analysis, and Optimization," *Structural and Multidisciplinary Optimization*, Vol. 59, 2019, pp. 1075–1104. https://doi.org/10.1007/s00158-019-02211-z.

[12] Hwang, J. T., and Martins, J. R., "A computational architecture for coupling heterogeneous numerical models and computing coupled derivatives," *ACM Transactions on Mathematical Software (TOMS)*, Vol. 44, No. 4, 2018, pp. 1–39.

[13] Hendricks, E. S., and Gray, J. S., "pycycle: A tool for efficient optimization of gas turbine engine cycles," *Aerospace*, Vol. 6, No. 8, 2019, p. 87.

[14] Nita, M., and Scholz, D., "Estimating the Oswald Factor from Basic Aircraft Geometrical Parameters," *Deutscher Luft- und Raumfahrtkongress*, Berlin, Germany, 2012.

[15] Raymer, D. P., "Aircraft design: a conceptual approach (AIAA Education Series)," *Reston, Virginia*, 2012.

[16] Chauhan, S. S., and Martins, J. R. R. A., "Low-Fidelity Aerostructural Optimization of Aircraft Wings with a Simplified Wingbox Model Using OpenAeroStruct," *Proceedings of the 6th International Conference on Engineering Optimization, EngOpt 2018*, Springer, Lisbon, Portugal, 2018, pp. 418–431. https://doi.org/10.1007/978-3-319-97773-7_38.

[17] Virtanen, P., Gommers, R., Oliphant, T. E., Haberland, M., Reddy, T., Cournapeau, D., Burovski, E., Peterson, P., Weckesser, W., Bright, J., et al., "SciPy 1.0: fundamental algorithms for scientific computing in Python," *Nature methods*, Vol. 17, No. 3, 2020, pp. 261–272.

[18] Gill, P. E., Murray, W., and Saunders, M. A., "SNOPT: An SQP algorithm for large-scale constrained optimization," *SIAM review*, Vol. 47, No. 1, 2005, pp. 99–131.

[19] Roskam, J., *Airplane design*, DARcorporation, 1985.

[20] Chiba, K., Obayashi, S., Nakahashi, K., and Morino, H., "High-fidelity multidisciplinary design optimization of aerostructural wing shape for regional jet," *23rd AIAA Applied Aerodynamics Conference*, 2005, p. 5080.